Virologica Sinica 37 (2022) 521–530

Contents lists available at ScienceDirect

Virologica Sinica

journal homepage: www.keaipublishing.com/en/journals/virologica-sinica
www.virosin.org

Research Article

ISG20 inhibits bluetongue virus replication

Di Kang [a], Shandian Gao [a], Zhancheng Tian [a], Guorui Zhang [a], Guiquan Guan [a], Guangyuan Liu [a], Jianxun Luo [a], Junzheng Du [a,*], Hong Yin [a,b,*]

[a] State Key Laboratory of Veterinary Etiological Biology, Lanzhou Veterinary Research Institute, Chinese Academy of Agricultural Sciences, Lanzhou, 730046, China
[b] Jiangsu Co-innovation Center for Prevention and Control of Important Animal Infectious Diseases and Zoonoses, Yangzhou University, Yangzhou, 225009, China

ARTICLE INFO

Keywords:
Bluetongue virus (BTV)
Interferon-stimulated genes (ISGs)
Ovine ISG20
Virus replication
Antiviral immunity

ABSTRACT

ISG20 is an interferon-inducible exonuclease that inhibits virus replication. Although ISG20 is thought to degrade viral RNA, the antiviral mechanism and specificity of ISG20 remain unclear. In this study, the antiviral role of ovine ISG20 (oISG20) in bluetongue virus (BTV) infection was investigated. It was found that BTV infection up-regulated the transcription of ovine ISG20 (oISG20) in a time- and BTV multiplicity of infection (MOI)-dependent manner. Overexpression of oISG20 suppressed the production of BTV genome, proteins, and virus titer, whereas the knockdown of oISG20 increased viral replication. oISG20 was found to co-localize with BTV proteins VP4, VP5, VP6, and NS2, but only directly interacted with VP4. Exonuclease defective oISG20 significantly decreased the inhibitory effect on BTV replication. In addition, the interaction of mutant oISG20 and VP4 was weakened, suggesting that binding to VP4 was associated with the inhibition of BTV replication. The present data characterized the anti-BTV effect of oISG20, and provides a novel clue for further exploring the inhibition mechanism of double-stranded RNA virus by ISG20.

1. Introduction

Bluetongue virus (BTV) is an arthropod-borne virus that is mainly transmitted by the biting midge (*Culicoides*) and causes bluetongue disease in ruminants. The disease is one of the major threats to the ruminant industry due to the high morbidity and mortality of livestock, especially sheep (Hilke et al., 2019). BTV belongs to the genus *Orbivirus* of the family *Reoviridae* and has been studied as a model of large, non-enveloped, double-stranded RNA (dsRNA) viruses. The outer capsid of BTV is composed of VP2 and VP5 proteins, which are responsible for cell attachment in the life cycle of the virus (Mohl and Roy, 2017). The inner capsid consists of VP3 and VP7 proteins, which encapsulate the helicase VP6, RNA polymerase VP1, capping enzyme VP4, and segments of dsRNA to make up the core particle of BTV (Patel and Roy, 2014). The non-structural proteins NS1~NS4 and NS3a are conserved among different types of BTVs and are necessary for viral replication. NS1 is sufficiently expressed in infected mammalian cells and functions to upregulate BTV encoded protein expression (Kerviel et al., 2019). NS2 is a component of viral inclusion bodies (VIBs) and can recruit BTV proteins and single-stranded RNA (ssRNA) to complete genomic packaging and core assembly (Rahman et al., 2020). NS3 and NS3a are the only membrane-associated proteins synthesized by BTV, which serve as key mediators of viral maturation and release via interacting with the face of VIBs (Beaton et al., 2002; Roy, 2008). Lastly, NS4 plays an important role in the antiviral response of host cells (Mohl and Roy, 2014; Labadie et al., 2020).

Innate immune responses in the host, including the production of type I interferon (IFN-I) and other inflammatory cytokines, are the first line of defense in combatting infection. These primitive responses play a crucial role in shaping the adaptive immune response (Shaw et al., 2017). Upon virus infection, the pathogen-associated molecular patterns of the pathogen can be detected by cellular sensors termed pattern recognition receptors, and then trigger a signaling cascade leading to the induction of IFN-α/β (Schoggins and Rice, 2011). The secreted IFN-α/β binds to the receptors IFNAR1 and IFNAR2 on the cell surface, followed by the activation of the JAK/STAT signal pathway. This is followed by hundreds of IFN-stimulated genes (ISGs) that are transcriptionally upregulated (Perng and Lenschow, 2018; Stetson and Medzhitov, 2006). Many ISGs have been reported to limit a variety of viruses at different stages of the viral life cycle, or regulate the immune response in host cells (Stetson and Medzhitov, 2006). In 1997, a gene encoding a 20 kDa protein, namely ISG20, was identified for the first time in different cell lines treated with IFN-I and IFN-II (Gongora et al., 1997). ISG20 was then recognized as a member of the DEDDh family of exonucleases and characterized as a viral

* Corresponding authors.
E-mail addresses: dujunzheng@caas.cn (J. Du), yinhong@caas.cn (H. Yin).

https://doi.org/10.1016/j.virs.2022.04.010
Received 29 August 2021; Accepted 22 April 2022
Available online 2 May 2022

inhibitor (Degols et al., 2007). This superfamily has both RNase and DNase activities in the presence of two divalent metal ions. The biochemical analyses demonstrated that ISG20 prefers to interact with the stem-loop at the 3′ end of ssRNA substrates. The 3′–5′ exonuclease activity of ISG20 is considered to be the dominant antiviral mechanism by degrading viral RNAs. The substitution of the conserved aspartic acid at position 94 to glycine would abolish exonuclease activity of ISG20 by more than 90%, thereby weakening the inhibitory effect on the virus (Nguyen et al., 2001; Zheng et al., 2017). For example, wild-type ISG20 inhibits human immunodeficiency virus (HIV), hepatitis A virus (HAV), and influenza virus while no antiviral effect was observed in mutant ISG20 overexpression cells. In addition to suppressing the proliferation of RNA viruses, ISG20 can also inhibits DNA viruses such as hepatitis B virus (HBV) and cytomegalovirus (Zhou et al., 2011; Espert et al., 2003, 2005; Hao and Yang, 2008; Simmen et al., 2001). In a study of ISG20 suppression of HBV, the interaction between the Exo III motif and the stem of the viral RNA resulted in HBV RNA degradation; therefore, both protein translation and DNA replication were inhibited (Liu et al., 2017). These data suggest that the contribution of ISG20 to defend against viral infections may vary (Espert et al., 2003).

After BTV infection, the expression of ovine ISG20 (oISG20) is significantly increased. This suggests that ISG20 may play an important role in anti-BTV infection (Du et al., 2016). Although BTV infection can be inhibited by IFN, the specific mechanism of IFN, especially involving ISGs, remains unclear (Vitour et al., 2014). In this study, we aimed to investigate the role of oISG20 in BTV infection. These data will provide an additional insight for the antiviral and biological function of oISG20.

2. Materials and methods

2.1. Cells and viruses

Baby hamster kidney 21 cells (BHK-21, ATCC-CCL-10) were cultured in modified Eagle's medium (Hyclone, USA) supplemented with 5% fetal bovine serum (FBS, Gibco, USA). HEK-293T cells obtained from China Center for Type Culture Collection (Shanghai, China) and ovine-derived kidney cells (MDOK, ATCC-CRL-1633) were maintained in Dulbecco's modified Eagle's medium (Gibco, USA) containing 10% FBS (Gibco, USA). The BTV-1 strain (GS/11) was propagated in BHK-21 cells. The virus titer was determined by the plaque formation assay and estimated as plaque forming units per milliliter (PFU/mL).

2.2. Virus infection

To investigate whether BTV infection could stimulate the transcription of oISG20, one group of MDOK cells was seeded onto 12-well plates for 12 h. Cultures were washed twice with serum-free DMEM and inoculated with the BTV-1 at a multiplicity of infection (MOI) = 0.1 for 1 h. The infected cells were collected at 0, 12, 24 and 48 h post-infection (hpi). The other group of MDOK cells was infected with an MOI = 0, 0.01, 0.1 and 1 for 48 h. Total RNA was extracted using Trizol Regent (Ambion, USA) following the manufacturer's instructions. The total RNA was then reverse-transcribed by PrimeScript RT reagent Kit with gDNA Eraser (TaKaRa, Japan) and quantitative real-time PCR (qRT-PCR) was performed to measure the expression of oISG20 mRNA level using TB Green®Premix ExTaq™II (TaKaRa, Japan). The qRT-PCR sequences of primers are shown in Supplementary Table S1. The procedure was performed using a real-time PCR system (Agilent, USA) and carried out with an initial incubation at 95 °C for 30 s, followed by 40 cycles of 5 s at 95 °C, and 30 s at 60 °C. The oISG20 mRNA was normalized by β-actin and the relative fold-changes were determined by the $2^{-\triangle\triangle CT}$ method.

2.3. Cloning and sequence analysis of oISG20 gene

The specific primers were designed according to the predicted mRNA sequence (XM_027957054) to obtain the CDS of oISG20 (Supplementary Table S1). MDOK cells were infected with BTV-1 at an MOI of 1 after culturing in 12-well plates. The cells were collected at 48 hpi. The total RNA was extracted using Trizol Regent and the RT-PCR was performed with One-step PrimeScript RT Reagent Kit (TaKaRa, Japan). The PCR products were ligated into the pMD-18T Vector (TaKaRa, Japan) and verified by DNA sequencing. The sequence alignment of ISG20 from different species was performed by the BioEdit software. The domains of oISG20 were analyzed using the Simple Modular Architecture Research Tool (SMART) (http://smart.embl-heidelberg.de/).

2.4. Plasmids

Primers were designed to subclone the CDS of oISG20 into pCAGGS-HA vector and the target gene would be expressed in fusion with the HA tag (Supplementary Table S1). The recombinant plasmid was named oISG20-HA. Since the exonuclease activity of ISG20 is an important source of its antiviral activity, an exonuclease-defective oISG20-expressing plasmid (termed mut-oISG20-HA) was constructed, in which aspartic acid at position 94 was mutated to glycine. Two pairs of primers were designed to obtain the full open reading frame of mutant oISG20: 1) from the first bp to the 283rd bp and the mutation site (281–283) is contained in the reverse primer, 2) amplify the fragment after the mutation site (283–516) (Supplementary Table S1). The two fragments were subcloned into the digested pCAGGS-HA using ClonExpress ® II One Step Cloning Kit (Vazyme, Nanjing). To explore the viral proteins that interact with the wild-type oISG20 and the mutant oISG20, the CDS of BTV VP1, VP2, VP3, VP4, VP5, VP6, and VP7 and NS1, NS2, and NS3 were subcloned into the pcDNA3.1 (−)-myc-His vector (Invitrogen, USA), respectively, which contains Myc- and His-tag in the N-terminal (Supplementary Table S1).

2.5. Transfection, knockdown, and viral infection

MDOK cells were seeded in 12-well plates and incubated for 16 h until cells grown on wells reached 80%~90% confluence. Then, the cells were transfected with 1.6 μg of pCAGGS-HA or oISG20-HA and mut-oISG20-HA by Lipofectamine ™ 3000 (Invitrogen, USA) following the manufacturer's instructions. At 24 hpi, MDOK cells were infected with BTV-1 at an MOI = 1. At various hpi (12, 24, and 48 hpi), the supernatant of the samples was collected to test the virus titers. Then, 1 mL of phosphate buffer saline (PBS) was added and the cells were scraped and collected. The cells in the pellet were harvested after centrifugation at 12,000×*g* for 10 min at 4 °C.

To investigate the effect of endogenous ISG20 on BTV replication, short interfering RNAs (siRNAs) were designed (the sequences of si-oISG20-1, −2, −3; shown in Supplementary Table S1) and synthesized by GenePharma, Shanghai. After MDOK cells were cultured in a 12-well plate for 16 h, 60 pmol of the si-oISG20-1, −2, −3 or negative control were transfected using RNAiMAX Transfection Reagent (ThermoFisher, USA) respectively. The transfected cells were infected with BTV-1 at an MOI of 1 and the sampling method was the same as mentioned above.

2.6. Quantitative real-time PCR

The total RNA was extracted from harvested cells by Trizol Reagent, and the cDNA was obtained as described above. The quantification of oISG20 and BTV was conducted by using TB Green®Premix ExTaq™II (TaKaRa, Japan) and specific primers (Supplementary Table S1). β-actin was the housekeeping gene used to normalize the target genes, and the relative RNA expression levels were determined using the $2^{-\triangle\triangle CT}$ method.

2.7. Immunoblot analysis

The protein content in the cellular pellet was separated on SDS-PAGE gels after cellular lysis and boiling for 10 min. The separated proteins

were transferred onto an Immobilon-P polyvinylidene difluoride (PVDF) membrane (Millipore, USA), followed by incubation in PBS containing 5% dried skim milk and 0.05% Tween-20 for 2 h at room temperature (RT). Membranes were incubated with the rabbit anti-NS1 and anti-VP6 antibody (prepared by our laboratory, 1:1000 dilution), mouse anti-HA-tag antibody (Proteintech, USA, 1:5000 dilution), and mouse anti-β-actin antibody (Bioworld, USA, 1:5000 dilution), respectively, for detection the expression of BTV NS1 and VP6 protein, oISG20, and β-actin. In the Co-IP assay, the expression of BTV VP1～VP7, NS1～NS3 was tested by the mouse anti-Myc-tag antibody (Cell Signaling Technology, USA, 1:1000 dilution). After overnight incubation at 4 °C, the membranes were washed with blocking buffer three times, and the membranes were incubated in HRP-conjugated goat-anti-mouse or goat-anti-rabbit secondary antibody (Abcam, USA, 1:10,000 dilution) for 1 h at RT. After membranes were washed, the bands were detected by using SuperSignal West Femto kit (Thermo, USA) in a ChemiDoc MP imaging system (Bio-Rad, USA). The band intensity was quantified by the Image J software.

2.8. Plaque assay

The virus titers of the cell culture supernatants of oISG20-HA, mut-oISG20-HA or pCAGGS-HA transfected cells, and the oISG20 knockdown cells, were determined by using a plaque formation assay. Briefly, BHK-21 cell monolayers grown in 24-well culture plates were incubated with serial dilutions of supernatants on a shaker table at RT. After 1 h, the inoculum was replaced with cell culture medium containing 1.5% low melting agarose (Invitrogen, USA) and cells were cultured for 2–3 days. The low melting agarose overlay was then removed and plaques were visualized via crystal violet stain. Plaques were counted manually and the number of PFU per mL was calculated.

2.9. Immunofluorescence assay

MDOK cells were grown on coverslips to 50% confluence and were co-transfected with BTV protein-expressing plasmids and oISG20-HA, or transfected with VP4, VP5, VP6, and NS2-expressing plasmids alone, then incubated for 24 h. Cells were fixed with 4% paraformaldehyde for 15 min after washing with PBS three times. Cells were permeabilized with 0.5% Triton X-100 for 10 min. Samples were then blocked with 3% bovine serum albumin (BSA) for 30 min and incubated with the primary antibody. VP1～VP3 were detected by the rabbit anti-His-tag antibody (ZSGB-Bio, China, 1:200 dilution), and VP4～VP7 were detected with rabbit anti-VP4～VP7 antibody (1:100 dilution), respectively. NS1～NS3 were detected with a rabbit anti-NS1～NS3 antibody (1:100 dilution) and mouse anti HA-tag (1:100 diluted) was used to test the expression of oISG20. All antibodies were diluted in PBS containing 1% BSA and samples were incubated overnight at 4 °C. After washing three times with PBS, cells were treated with Alexa Fluor-conjugated goat anti-rabbit or goat anti-mouse secondary antibody (Abcam, USA, 1:1000 dilution) for 1 h at RT in the dark. Following washing steps, samples were incubated with Hoechst 33,342 (Sigma-Aldrich, USA) for 10 min at RT and mounted. Images were obtained using a confocal microscope (Leica, Germany).

2.10. Co-immunoprecipitation (Co-IP)

HEK-293T cells were co-transfected with Myc- and His -tagged BTV proteins and HA-tagged oISG20 or mut-oISG20-HA plasmids using lipofectamine 3000 (Invitrogen, USA) in accordance with the manufacturer's instructions. After culturing for 48 h, the cells were washed with cold PBS and lysed using NP-40 buffer with protease inhibitors for 30 min (Beyotime, China). The cell lysates were centrifuged at 13,000×*g* for 10 min at 4 °C and the pellet was discarded. Then, 60 μL of the cell lysate was saved for input control and added 10 μg of the immunoprecipitation antibody into the rest of the lysate, then incubated overnight at 4 °C with gentle shaking. Next, 30 μL of precleared protein G agarose (Sigma, USA) was added to the reaction mixture with gentle shaking for 3 h at 4 °C. The bead-bound antibody-protein complexes were washed by slow centrifugation in NP-40 buffer five times. For the Western blot analysis, the purified beads were eluted in SDS-PAGE buffer and boiled for 10 min.

3. Results

3.1. BTV infection stimulates oISG20 transcription

To examine the level of oISG20 transcription after BTV infection, the total RNA was extracted from BTV-infected MDOK cells. The qRT-PCR results showed that oISG20 transcription was up-regulated after BTV infection, which continued for 48 h after infection, reaching up to 36-fold higher than the uninfected cells at 48 hpi (Fig. 1A). As shown in Fig. 1B, the oISG20 mRNA expression was BTV MOI-dependent. Compared with cells without BTV infection, the expression of oISG20 mRNA in cells infected with an MOI of 0.01, 0.1 and 1, increased by 4.84-, 38.42- and 182.88-fold, respectively.

3.2. Sequence analysis of oISG20

We successfully amplified the CDS of *oISG20* gene from BTV infected MDOK cells. The open reading frame of the oISG20 comprises 513 nucleotides encoding 171 amino acids with a predicted molecular mass of 20.43 kDa. Similar to ISG20s found in other species, oISG20 contains three exonuclease domains: Exo I from 7 to 16 amino acids, Exo II from 86 to 102 AA, and Exo III from 147 to 157 AA (Fig. 2). To better

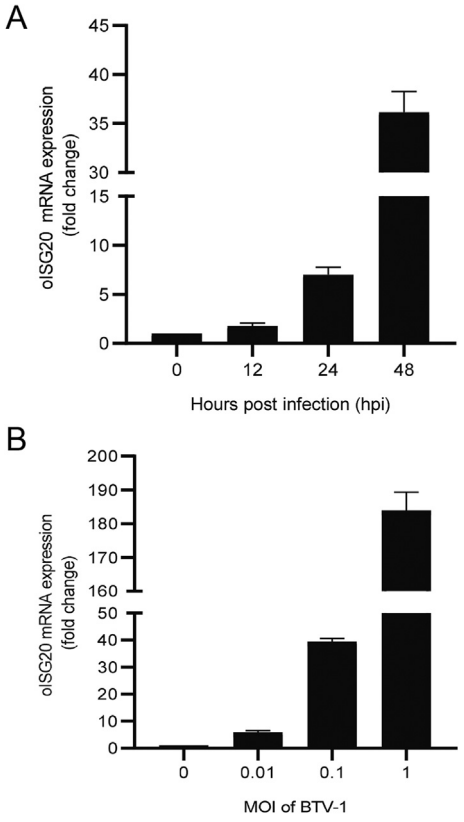

Fig. 1. Stimulation of oISG20 mRNA by BTV infection. **A** ISG20 mRNA production gradually increased over time. The MDOK cells were infected with BTV-1 with an MOI = 0.1, and at 12, 24 and 48 hpi, cells were harvested to measure the oISG20 mRNA using qRT-PCR. **B** MDOK cells were infected with BTV-1 at an MOI = 0, 0.01, 0.1, and 1, and the mRNA of oISG20 was determined by qRT-PCR at 48 hpi. The relative fold changes were determined by the $2^{-\triangle\triangle CT}$ method.

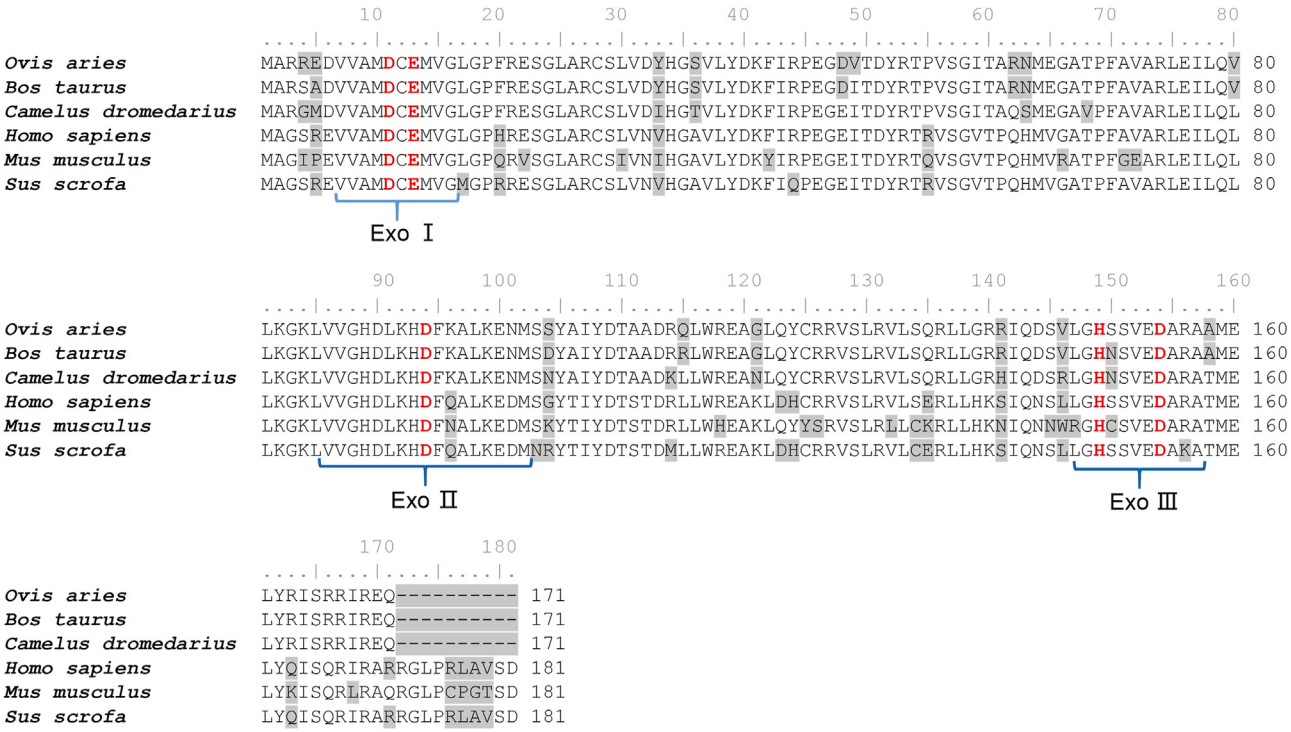

Fig. 2. Amino acid sequence alignment of mammalian ISG20. Different amino acids are shaded in grey. The three exonuclease active motifs Exo I, II, and III of ISG20 are marked by brackets below the sequences. The conserved amino acid residues from the DEDDh family are in bold and highlighted in red letters.

understand the sequence identity of oISG20 compared with other species, sequence alignment was performed by protein BLAST in NCBI. The results indicated that oISG20 showed a relatively higher AA sequence identity with ruminants such as goat (97.66%), cattle (96.94%), alpaca (89.47%) and camel (89.47%) than non-ruminants, and the identity with dog ISG20 at 82.25%, cat ISG20 at 79.88% and human at 78.70%. Boar, rabbit, and mouse ISG20 was found to be 75.17%, 73.37%, and 70.76% identical with the oISG20, respectively (Table 1).

3.3. oISG20 overexpression restricts BTV replication

To evaluate the role of oISG20 during BTV infection, cells transfected with either oISG20 or pCAGGS-HA for 24 h were infected with BTV. The production of BTV proteins, viral genome, and virus titers were measured by Western blot analysis, qRT-PCR, and plaque assay, respectively. The results showed that NS1 and VP6 proteins were decreased in oISG20-HA transfected cells, compared with pCAGGS-HA transfected cells (Fig. 3A). Moreover, oISG20 overexpression induced a reduction in the level of NS3 RNA, which was down-regulated by an average of 0.85-, 0.63-, and 0.5-fold at 12, 24, and 48 hpi, respectively (Fig. 3B). The supernatant of these samples was collected to test the infectious particles by using the plaque assay. The results showed that the virus titers in pCAGGS-HA-transfected cells were approximately 2.2-, 1.58-, and 2.05-fold greater than oISG20-HA transfected cells at 12, 24, and 48 hpi, respectively (Fig. 3C).

Table 1
The identity of oISG20 with other ISG20s.

Scientific Name	Common Name	Accession Number	Size (AAs)	Identity (%) With oISG20
Capra hircus	Goat	XP_005694999.1	171	97.66
Bos taurus	Cattle	XP_002696560.1	171	96.94
Vicugna pacos	Alpaca	XP_006198618.2	171	89.47
Camelus dromedarius	Camel	XP_010974031.1	171	89.47
Canis lupus familiaris	Dog	XP_545847.2	171	82.25
Felis catus	Cat	XP_019687460.1	171	79.88
Homo sapiens	Human	CAG33223.1	181	78.70
Sus scrofa	Boar	AAU09455.2	181	75.17
Oryctolagus cuniculus	Rabbit	XP_017195951.1	181	73.37
Mus musculus	Mouse	CAJ18421.1	181	70.76

3.4. Knockdown of oISG20 enhances the BTV production

The specific siRNAs were designed to target different segments of oISG20 mRNA to explore whether endogenous oISG20 had antiviral activity against BTV (Supplementary Table S1). The knockdown efficiency of si-oISG20-1, si-oISG20-2, and si-oISG20-3 was 54.75%, 41.31%, and 71.30%, respectively (Fig. 4A). MDOK cells were infected with BTV following transfection with specific siRNAs or NC for 24 h. The BTV protein expression levels in cell lysates were determined by immunoblotting. Obvious differences between the siRNA interference groups and the control cells were detected. The results showed that the expression of the NS1 and VP6 proteins in the cells transfected with three groups of different siRNAs was obviously increased (Fig. 4B). The NS3 RNA level in oISG20 knockdown cells were 1.48-, 1.1-, and 4.47-fold greater than in the NC group (Fig. 4C). Cell culture was collected to determine the mature virion production. The data indicated that the viral titers in oISG20 knockdown cells were 1.37-, 1.16-, and 1.47-fold greater than the NC transfected cells (Fig. 4D).

3.5. The confocal and interaction assay between oISG20 and BTV proteins

To investigate the potential mechanism of oISG20 inhibiting BTV replication, the intracellular locations of ten viral proteins were analyzed by co-transfecting oISG20-HA with BTV proteins in MDOK cells or not. It was observed that ISG20 was mainly distributed in the cytoplasm of MDOK cells, and VP4, VP5, VP6, and NS2 were co-located with oISG20. In contrast, other six proteins including VP1, VP2, VP3, VP7, NS1, and NS3 were not co-located with oISG20. VP4 and VP5 tended to accumulate near the cytoplasm membrane, and VP6 and NS2 were largely localized in the cytoplasm (Fig. 5). In addition, when oISG20 was co-expressed with these four viral proteins, their localization was not apparently altered.

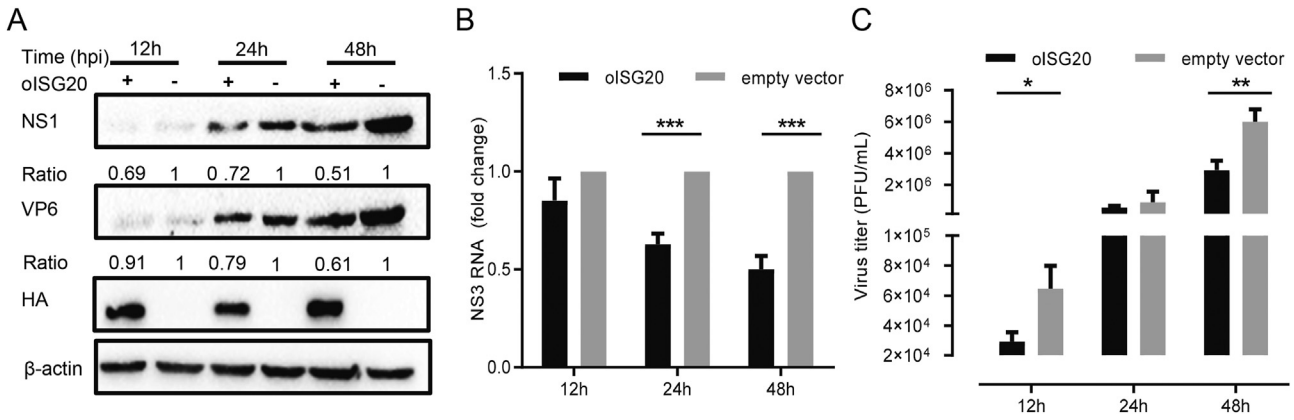

Fig. 3. The overexpression of oISG20 inhibits BTV replication. **A** Detection of NS1 and VP6 protein expression by Western blot after oISG20 transfection and BTV infection. Cell lysates were harvested at 12, 24, and 48 hpi and the expression of oISG20 was detected with an anti-HA tag antibody. The relative intensity of NS1 and VP6 to pCAGGS-HA transfected group at different time points are marked below the bands. **B** The relative levels of NS3 RNA were measured in the overexpression of oISG20 or not. β-actin was used as a housekeeping gene to normalize the target gene. **C** Plaque assay showing the virus titer in cell cultures infected with BTV-1 after transfected by either oISG20-HA or pCAGGS-HA. Error bars represent the means ± S.D. of the data from three independent experiments. Differences between the oISG20-overexpressing and pCAGGS-HA transfected groups are marked with * ($P < 0.05$); ** ($P < 0.01$); or *** ($P < 0.001$).

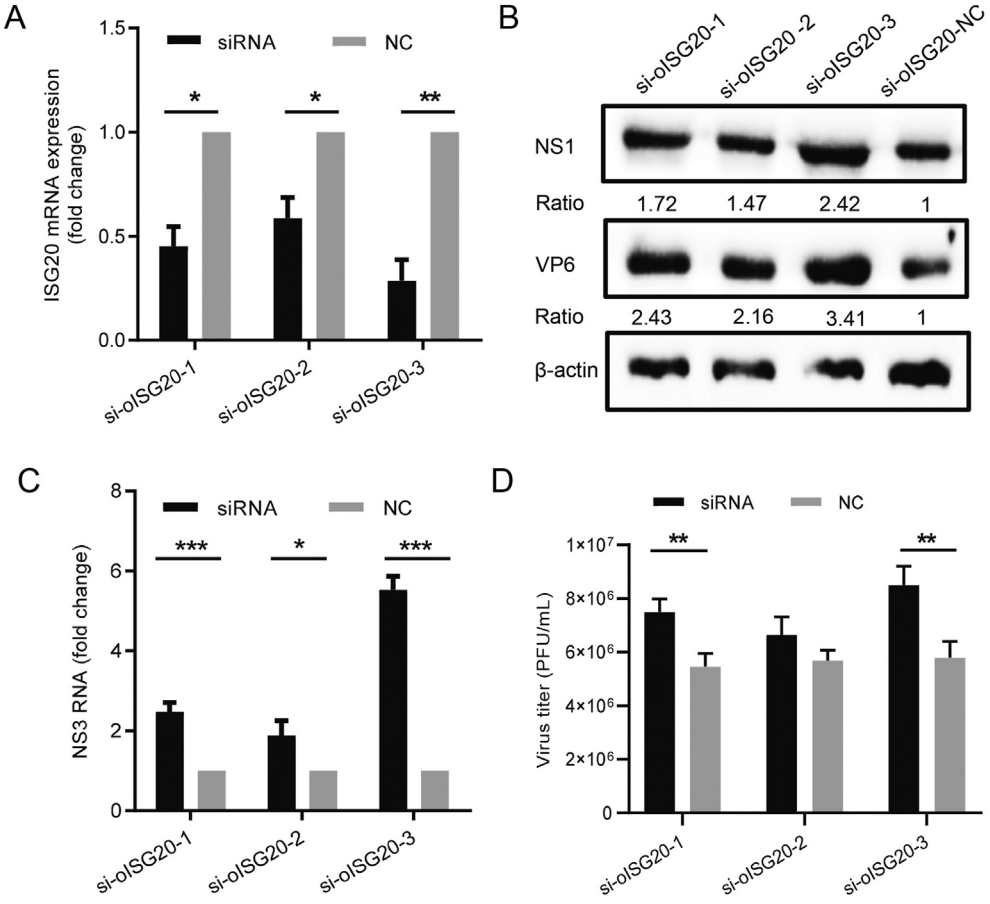

Fig. 4. Knockdown of oISG20 increased the replication of BTV. **A.** The efficiency of knockdown by three pairs of siRNA transfection. The MDOK cells were transfected with si-oISG20-1, si-oISG20-2, and si-oISG20-3 respectively for 48 h. Samples were collected to determine the expression of oISG20 mRNA by qRT-PCR. The target gene was normalized to β-actin. **B.** BTV proteins in the cell lysate were detected by Western blot. MDOK cells were incubated for 24 h after the siRNA transfection, then infected with BTV-1 at an MOI = 1. Samples were collected at 48 hpi. The relative intensity of NS1 and VP6 to the pCAGGS-HA transfected group at different time points are marked below the bands. **C.** The relative change of NS3 RNA levels in oISG20 knockdown cells was tested by qRT-PCR after BTV infection for 48 h. **D.** The virus titers in the supernatant were assessed at 48 hpi by plaque assay on BHK-21 cells. Error bars represent the means ± S.D. of data from three independent experiments. *, $P < 0.05$; **, $P < 0.01$; ***, $P < 0.001$.

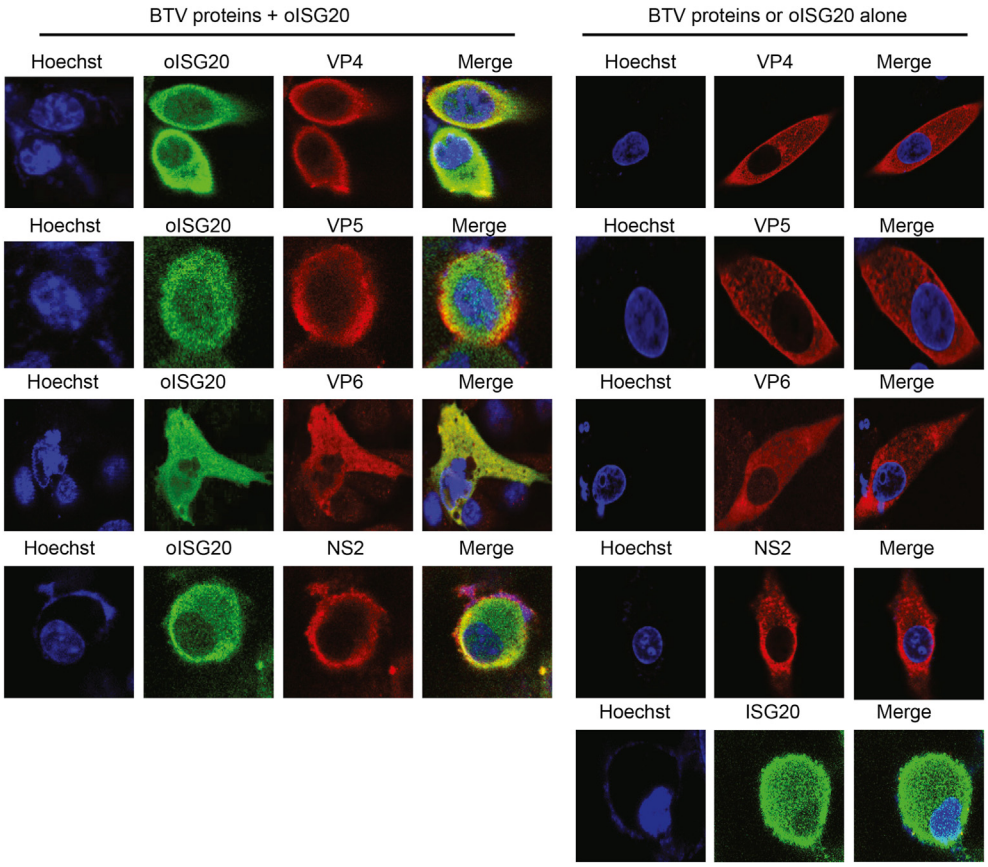

Fig. 5. oISG20 colocalized with VP4, VP5, VP6, and NS2. MDOK cells were co-transfected with BTV protein-expressing plasmids and oISG20-HA or not. After incubation for 24 h at 37 °C, cells were stained with a mouse anti-HA antibody, rabbit anti-His-tag antibody, and rabbit anti-BTV protein antibody. Nuclei were stained with Hoechst (blue). Expression and the locations were analyzed by confocal microscopy. The magnification of confocal microscope is 100×.

Co-IP experiments were performed to test the interaction of oISG20 with viral proteins. As mentioned above, target proteins were transiently expressed in HEK-293T cells by co-transfection. The results showed that Myc- and His-tagged VP4 was detected after immunoprecipitation with the anti-HA antibody. However, other viral proteins, especially VP5, VP6, and NS2 did not co-precipitated with oISG20 (Fig. 6A). The reverse immunoprecipitation experiment showed that only Myc-tagged VP4 pulled down the HA-tagged oISG20, which indicated the direct interaction between oISG20 and BTV VP4 protein (Fig. 6B).

3.6. The inhibitory effect of mutant oISG20 on BTV replication

Since the exonuclease domain of ISG20 may be important for its antiviral activity, the exonuclease defective mutant oISG20 plasmid, in which aspartic acid at position 94 was mutated to glycine, was constructed. Both oISG20-HA and mut-oISG20-HA were transfected into MDOK cells to achieve overexpression, respectively, then after 24 h, the cells were infected with BTV. The difference in BTV suppression between wild-type and mutant oISG20 was observed and compared at 24 and 48 hpi by measuring BTV proteins, viral genome, and viral titer in the supernatant.

The immunoblot results demonstrated that the expression of NS1 and VP6 proteins in cells transfected with mut-oISG20-HA and oISG20-HA decreased in varying degrees compared to the pCAGGS-HA-transfected group. In addition, the production of viral proteins in oISG20 overexpressing cells was less than that in mut-oISG20-HA transfected cells (Fig. 7A–C). The decrease of NS3 RNA in the ISG20 overexpressed group was 22% and 24% higher than mut-oISG20-HA transfected cells at 24 and 48 hpi, respectively (Fig. 7D). The virus titers of oISG20-expressing cells decreased by 61.8% and 59.7% at 24 and 48 hpi, but the virus titers in mut-ISG20-HA transfected samples were 33.5% and 20.8% less than vector-transfected groups (Fig. 7E). Interestingly, the virus protein and titers in mut-oISG20-HA transfected cells had a significant difference compared with oISG20-HA transfected cell except NS1 expression at 24 hpi (Fig. 7B, C and E), whereas the level of NS3 RNA had no difference in both groups (Fig. 7D).

We further co-expressed VP4 along with either oISG20-HA or mut-oISG20-HA in HEK-293T cells. It was found that mutant oISG20 could also interact with the VP4 protein, but the band intensity of the immunoprecipitated products in mutant oISG20 expressing cells was obviously reduced, compared with wild-type ISG20 overexpressing cells (Fig. 7F). The results indicated that the interaction with mutant oISG20 was weaker than that with wild-type oISG20, and the 94D of ExoII may play a role in inhibiting the production of viral proteins by interacting with VP4 instead of degrading the viral RNA.

4. Discussion

The expression of ISG20 can be stimulated by type I and type II IFN, poly I:C, and viral infection (Gongora et al., 1997). Recent research has shown that ISGs were significantly upregulated by BTV infection (Du et al., 2016; Ruscanu et al., 2012). In our study, oISG20 was induced rapidly and strongly in MDOK cells after BTV infection. The transcription of oISG20 was shown in both a time- and BTV MOI-dependent manner, suggesting that oISG20 plays an important role in the process of BTV infection. This result is similar to that observed in the infection of HIV in Human T-lymphoblastoid CEM cells where ISG20 expression gradually increased within 24 h post-infection (Espert et al., 2005). However, ISG20 was induced in liver cells during HBV clearance instead of viral entry and expansion (Wieland et al., 2004). These data suggested that

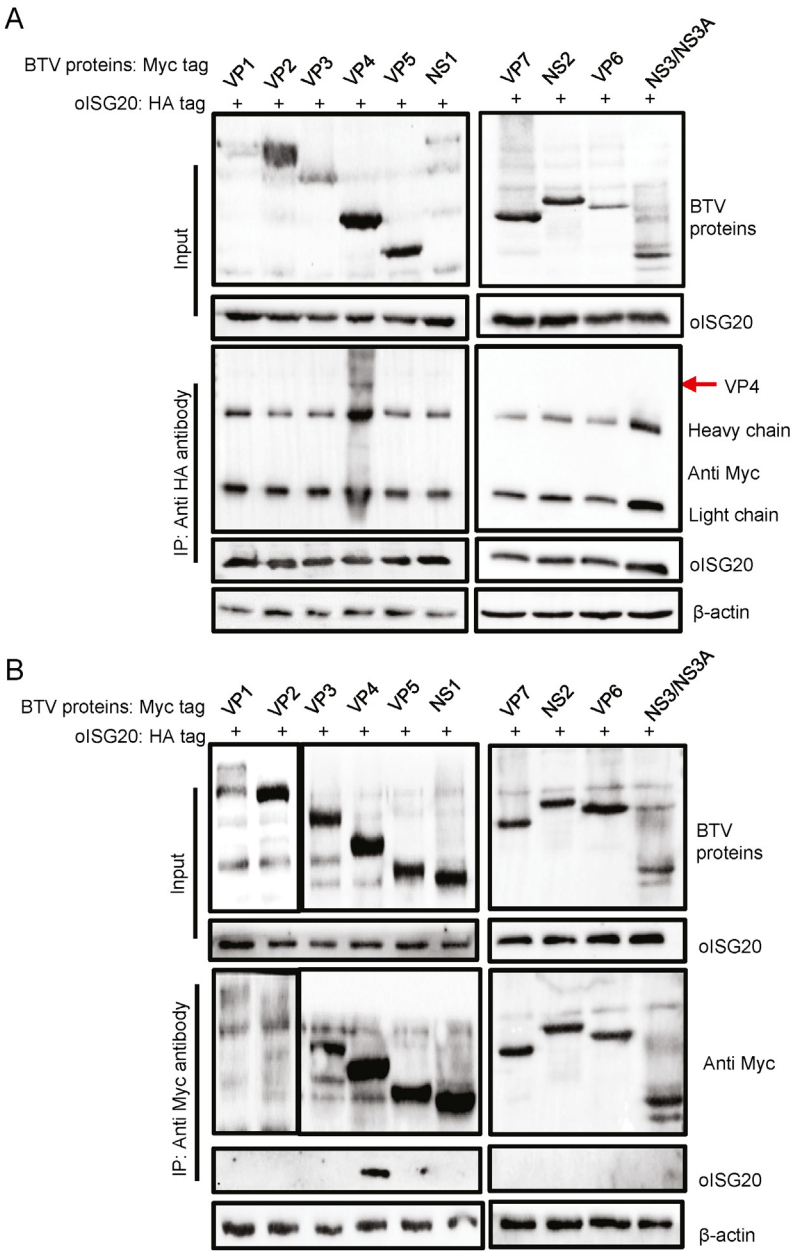

Fig. 6. The interaction between oISG20 and BTV proteins. **A** Immunoprecipitation analysis of HEK-293T cells transfected with oISG20-HA along with plasmids expressing BTV proteins. Whole-cell lysates (input) and the immunoprecipitated proteins were detected by immunoblotting using anti-Myc and anti-HA antibodies. The light chain (25 kDa) and heavy chain (55 kDa) of the HA antibody (IP antibody) were detected in the results of immunoprecipitation. **B** Similar transfection in HEK-293T cells and Co-IP experiments were performed as described above. However, the lysates were immunoprecipitated with an anti-Myc antibody. The input levels of β-actin were used as the loading controls.

stimulation and expression of ISG20 is variable among different viral infections.

To investigate the characteristics of the oISG20 sequence, the CDS was amplified and analyzed. It was found that the sequences of ISG20 are conserved among ruminants. oISG20 showed a higher identity with non-ruminants compared with other ISGs, for instance, ovine IFIT1 shares a 65% identity with humans, 67% with mice, and 70% with pandas, whereas oISG20 exceeded 70% in the present study. Three exonuclease motifs termed ExoI, ExoII, and ExoIII were found in oISG20. The key positions of exonuclease enzyme activity were the same as those found in humans, mice, and swine even while lacking ten amino acids at the C-terminal. Interestingly, many ISG20s seem to consist of only a unique exonuclease catalytic domain, without obvious regulatory domains. This may suggest that the regulation of ISG20 is the result of a variety of factors. Enzyme activity may be specifically exerted in the local environment while avoiding non-specific host RNA degradation (Degols et al., 2007).

Since the discovery of ISG20 as an interferon-induced RNase, its function in innate immune response has been widely studied (Gongora et al., 1997; Zheng et al., 2017). However, the antiviral mechanism of ISG20 on many viruses is not well understood. In this study, the inhibitory activity of oISG20 was studied by evaluating the effect of either overexpression or knockdown of oISG20 on BTV replication. The results showed that oISG20 significantly suppressed NS1 and VP6 expression,

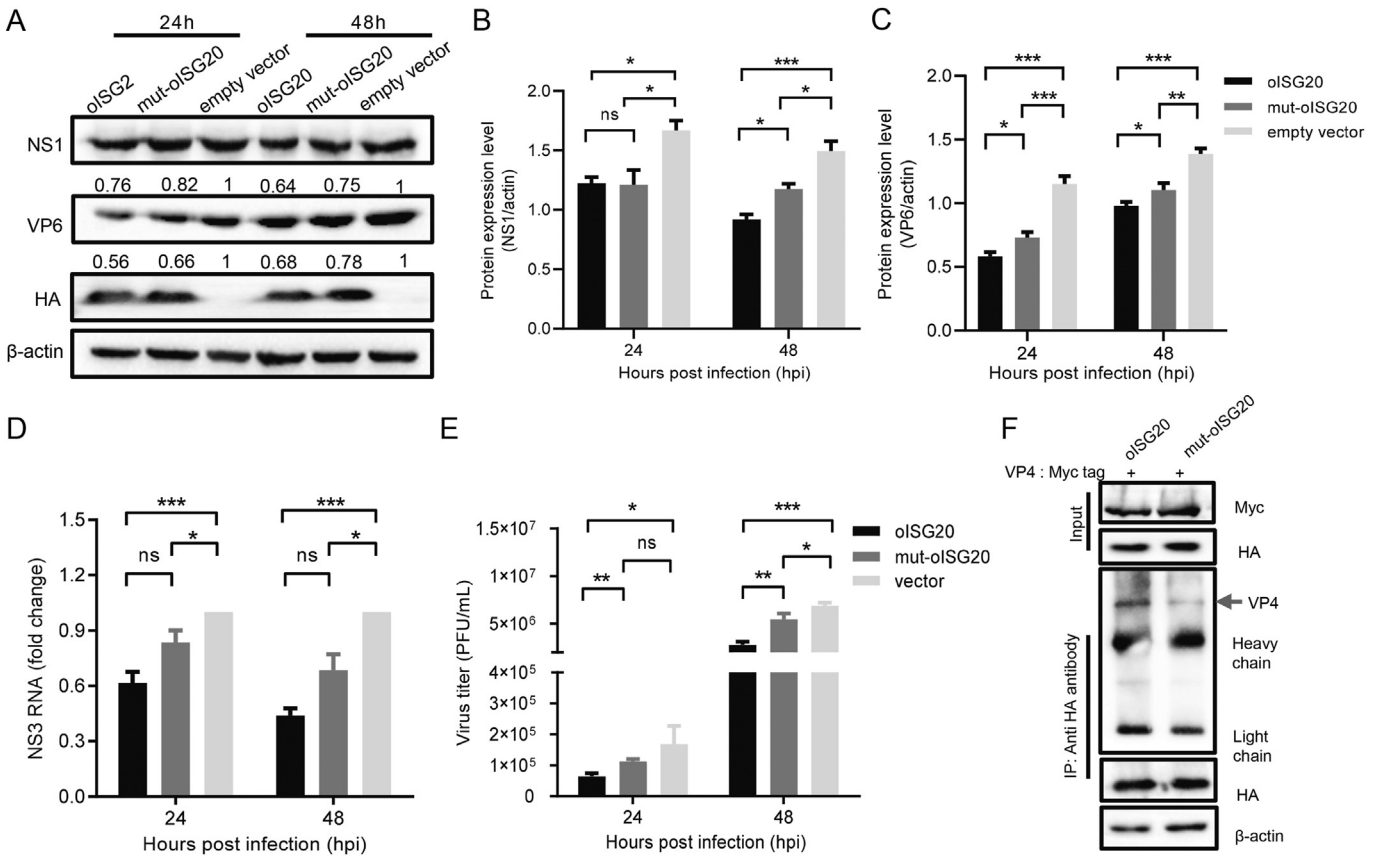

Fig. 7. The anti-BTV activity of the mutant oISG20 and the interaction with VP4 was weaker than ISG20. **A.** BTV protein production in mutant oISG20 overexpressed cells was higher than oISG20 overexpressed cells. MDOK cells were infected with BTV at an MOI = 1 after transfection with oISG20-HA, mut-oISG20-HA, and pCAGGS-HA for 24 h. NS1 and VP6 production of cell lysate was tested by immunoblotting. The relative intensity of NS1 and VP6 to the pCAGGS-HA-transfected group at different hpi was marked below the bands. **B** and **C**. Band quantification in A was performed using Image J software. The intensity of β-actin was used for normalization. **D.** The levels of NS3 RNA in the oISG20-HA, mut-oISG20-HA or pCAGGS-HA-transfected cells were measured by qRT-PCR with β-actin as the control. **E** Virus titers in the cell culture of oISG20-HA, mut-oISG20-HA or pCAGGS-HA transfected cells. **F.** The BTV-1 VP4 expressing plasmid was co-transfected with oISG20-HA or mut-oISG20-HA into HEK293T cells. After 48 h, cells were lysed and analyzed by immunoprecipitation and Western blot. Means ± S.D. of data from three independent experiments is shown in error bars. *, $P < 0.05$; **, $P < 0.01$; ***, $P < 0.001$; ns, not significant.

viral genome, and virus titers in oISG20-HA transfected MDOK cells. Similarly, Jiang et al. (2008) showed that hepatitis C virus (HCV) RNA was reduced by more than half in a stable cell line overexpressing ISG20, and the production of NS5A protein was also decreased at the same time (Jiang et al., 2008). The replication of some flaviviruses was repressed in Huh 7.5-derived cells caused by ISG20 overexpression, including bovine viral diarrhea-mucosal disease virus, West Nile virus, and Dengue virus. However, in some viruses such as SARS-CoV-1, ISG20 did not exhibit antiviral activity (Zhou et al., 2011). In the present study, the three small interfering RNAs had different interference efficiencies on oISG20 expression. si-oISG20-3 demonstrated the most efficient oISG20-knockdown activity, which mostly increased BTV infection. These data demonstrate that both overexpressed and endogenous ISG20 have inhibitory effects on BTV propagation.

The colocation and interaction between virus and host proteins usually offer clues to elucidating the antiviral mechanism of ISGs. For example, ISG20 has been found to interact with influenza A viral nucleoprotein to block the translation of viral proteins thereby facilitating antiviral activity (Qu et al., 2016). Thus, BTV protein-expressing plasmids were constructed to screen proteins that interact with oISG20. It was found that oISG20 co-localized with VP4, VP5, VP6, and NS2 in the cytoplasm, and the overexpression of oISG20 did not alter the location of the BTV proteins, indicating that the inhibitory effect of oISG20 may function outside the nucleus. In addition, ISG20 is a small, soluble protein that functions as an RNA modifier, it might freely diffuse through the nuclear pore complex as it was found that oISG20 localized to the nucleus. (Weiss et al., 2018). The Co-IP assay confirmed the co-location of oISG20 and VP4, but the interaction between oISG20 and VP5, VP6, or NS2 was not detected. The interaction between mutant oISG20 and VP4 was obviously decreased, indicating that this conserved 94D of ExoII is an important site for the interaction. However, the exact interaction sites of oISG20 and VP4, and whether oISG20 interacts with VP5, VP6, and NS2 via other factors remains to be further studied.

VP1, VP4, and VP6 consist of BTV transcriptase complexes, which are activated by the removal of the outer capsid and subsequently initiate the synthesis of ssRNA from the dsRNA genome (Mertens et al., 2004). VP4 serves as a capping enzyme in the 5′ terminus of the BTV transcript to take advantage of the translation machinery of host cells (Mohl and Roy, 2014). The difference in the viral titer and protein between the mutant and wild-type oISG20 overexpressed cells was higher than that of viral RNA. We speculate that the reason for this is that the interaction between oISG20 and VP4 disrupted VP4 functionality in the production of mature ssRNA, which subsequently suppressed the effectiveness of viral translation and assembly. The force of the interaction between mutant oISG20 and VP4 was weakened, which resulted in a weaker impact on VP4 activity and virus assembly. Therefore, the viral translation level and virus titer in mutant oISG20 overexpressed cells were obviously higher than in oISG20 overexpressed cells. Since NS1 is a very early protein expressed with the largest abundance in BTV-infected, it was speculated that the effect of ISG20 inhibition on NS1 was observed later than other viral proteins. Except for the inhibitory effects demonstrated in this research, oISG20 may have alternate methods of repressing BTV replication. For

example, the ISG20 target of Kaposi's sarcoma-associated herpesvirus (KSHV) microRNAs may inhibit inflammatory cytokines to downregulate virus replication (Dai et al., 2016). ISG20 exhibiting defective enzyme activity has been found to dramatically interrupt the ability of IFN, which blocked VSV but not EMCV or influenza virus replication. These data indicate that the exonuclease site is important for inducing the IFN response of VSV infection, with only a minor contribution in EMCV and influenza virus infection (Espert et al., 2003). The mutant ISG20 still displayed an inhibitory effect on BTV replication, though much weaker than wild-type ISG20. It is possible that oISG20 inhibits the BTV infection by other mechanisms. However, the specific antiviral mechanism that involves the interaction between VP4 and oISG20 in inhibiting BTV infection requires further investigation.

5. Conclusions

In conclusion, the data presented here give a brief analysis of the oISG20 sequence. The effect of oISG20 on BTV infection in MDOK cells was evaluated. By overexpression and knockdown experiments, it was found that oISG20 inhibited BTV replication at the level of viral protein production, viral genome, and virus titer. The 94D of oISG20 was important for the interaction with VP4, which may be related to the inhibitory effect of oISG20 on BTV proliferation. These results provide novel insight into understanding the antiviral mechanism of ISG20 and the development of a novel strategy for the treatment of Bluetongue.

Data availability

The authors declare that the data supporting the findings of this study are available within the article or upon request to the corresponding authors.

Ethics statement

This article does not contain any studies with human or animal subjects performed by any of the authors.

Author contributions

Di Kang: investigation, data curation, writing-original draft. Shandian Gao: data curation, methodology and writing – review & editing. Zhancheng Tian: data curation and methodology. Guorui Zhang: investigation and data curation. Guiquan Guan, Guangyuan Liu and Jianxun Luo: formal analysis and methodology. Junzheng Du and Hong Yin: conceptualization, methodology, writing – review & editing, supervision.

Conflict of interest

The authors declare that they have no conflict of interest.

Acknowledgements

This study was financially supported by the National Key Research and Development Program of China (2021YFD1800502; 2017YFD0502304); National Natural Science Foundation of China (31672562); NBCITS (CARS-37); ASTIP (CAAS-ASTIP-2016-LVRI); Jiangsu Co-innovation Center Program for the Prevention and Control of Important Animal Infectious Diseases and Zoonoses.

Appendix A. Supplementary data

Supplementary data to this article can be found online at https://doi.org/10.1016/j.virs.2022.04.010.

References

Beaton, A.R., Rodriguez, J., Reddy, Y.K., Roy, P., 2002. The membrane trafficking protein calpactin forms a complex with bluetongue virus protein NS3 and mediates virus release. Proc. Natl. Acad. Sci. U. S. A. 99, 13154–13159.
Dai, L., Bai, L., Lin, Z., Qiao, J., Yang, L., Flemington, E.K., Zabaleta, J., Qin, Z., 2016. Transcriptomic analysis of KSHV-infected primary oral fibroblasts: the role of interferon-induced genes in the latency of oncogenic virus. Oncotarget 7, 47052–47060.
Degols, G., Eldin, P., Mechti, N., 2007. ISG20, an actor of the innate immune response. Biochimie 89, 831–835.
Du, J., Xing, S., Tian, Z., Gao, S., Xie, J., Chang, H., Liu, G., Luo, J., Yin, H., 2016. Proteomic analysis of sheep primary testicular cells infected with bluetongue virus. Proteomics 16, 1499–1514.
Espert, L., Degols, G., Gongora, C., Blondel, D., Williams, B.R., Silverman, R.H., Mechti, N., 2003. ISG20, a new interferon-induced RNase specific for single-stranded RNA, defines an alternative antiviral pathway against RNA genomic viruses. J. Biol. Chem. 278, 16151–16158.
Espert, L., Degols, G., Lin, Y.L., Vincent, T., Benkirane, M., Mechti, N., 2005. Interferon-induced exonuclease ISG20 exhibits an antiviral activity against human immunodeficiency virus type 1. J. Gen. Virol. 86, 2221–2229.
Gongora, C., David, G., Pintard, L., Tissot, C., Hua, T.D., Dejean, A., Mechti, N., 1997. Molecular cloning of a new interferon-induced PML nuclear body-associated protein. J. Biol. Chem. 272, 19457–19463.
Hao, Y., Yang, D., 2008. Cloning, eukaryotic expression of human ISG20 and preliminary study on the effect of its anti-HBV. J. Huazhong Univ. Sci. Technol. Med. Sci. 28, 11–13.
Hilke, J., Strobel, H., Woelke, S., Stoeter, M., Voigt, K., Moeller, B., Bastian, M., Ganter, M., 2019. Presence of antibodies against bluetongue virus (BTV) in sheep 5 to 7.5 Years after vaccination with inactivated BTV-8 vaccines. Viruses 11, 533.
Jiang, D., Guo, H., Xu, C., Chang, J., Gu, B., Wang, L., Block, T.M., Guo, J.T., 2008. Identification of three interferon-inducible cellular enzymes that inhibit the replication of hepatitis C virus. J. Virol. 82, 1665–1678.
Kerviel, A., Ge, P., Lai, M., Jih, J., Boyce, M., Zhang, X., Zhou, Z.H., Roy, P., 2019. Atomic structure of the translation regulatory protein NS1 of bluetongue virus. Nat. Microbiol. 4, 837–845.
Labadie, T., Sullivan, E., Roy, P., 2020. Multiple routes of bluetongue virus egress. Microorganisms 8, 965.
Liu, Y., Nie, H., Mao, R., Mitra, B., Cai, D., Yan, R., Guo, J.T., Block, T.M., Mechti, N., Guo, H., 2017. Interferon-inducible ribonuclease ISG20 inhibits hepatitis B virus replication through directly binding to the epsilon stem-loop structure of viral RNA. PLoS Pathog. 13, e1006296.
Mertens, P.P., Diprose, J., Maan, S., Singh, K.P., Attoui, H., Samuel, A.R., 2004. Bluetongue virus replication, molecular and structural biology. Vet. Ital. 40, 426–437.
Mohl, B.P., Roy, P., 2014. Bluetongue virus capsid assembly and maturation. Viruses 6, 3250–3270.
Mohl, B.P., Roy, P., 2017. Elucidating virus entry using a tetracysteine-tagged virus. Methods 127, 23–29.
Nguyen, L.H., Espert, L., Mechti, N., Wilson 3rd, D.M., 2001. The human interferon- and estrogen-regulated ISG20/HEM45 gene product degrades single-stranded RNA and DNA in vitro. Biochemistry 40, 7174–7179.
Patel, A., Roy, P., 2014. The molecular biology of Bluetongue virus replication. Virus Res. 182, 5–20.
Perng, Y.C., Lenschow, D.J., 2018. ISG15 in antiviral immunity and beyond. Nat. Rev. Microbiol. 16, 423–439.
Qu, H., Li, J., Yang, L., Sun, L., Liu, W., He, H., 2016. Influenza A Virus-induced expression of ISG20 inhibits viral replication by interacting with nucleoprotein. Virus Gene. 52, 759–767.
Rahman, S.K., Kerviel, A., Mohl, B.P., He, Y., Zhou, Z.H., Roy, P., 2020. A calcium sensor discovered in bluetongue virus nonstructural protein 2 is critical for virus replication. J. Virol. 94, e01099-20.
Roy, P., 2008. Functional mapping of bluetongue virus proteins and their interactions with host proteins during virus replication. Cell Biochem. Biophys. 50, 143–157.
Ruscanu, S., Pascale, F., Bourge, M., Hemati, B., Elhmouzi-Younes, J., Urien, C., Bonneau, M., Takamatsu, H., Hope, J., Mertens, P., Meyer, G., Stewart, M., Roy, P., Meurs, E.F., Dabo, S., Zientara, S., Breard, E., Sailleau, C., Chauveau, E., Vitour, D., Charley, B., Schwartz-Cornil, I., 2012. The double-stranded RNA bluetongue virus induces type I interferon in plasmacytoid dendritic cells via a MYD88-dependent TLR7/8-independent signaling pathway. J. Virol. 86, 5817–5828.
Schoggins, J.W., Rice, C.M., 2011. Interferon-stimulated genes and their antiviral effector functions. Curr. Opin. Virol. 1, 519–525.
Shaw, A.E., Hughes, J., Gu, Q., Behdenna, A., Singer, J.B., Dennis, T., Orton, R.J., Varela, M., Gifford, R.J., Wilson, S.J., Palmarini, M., 2017. Fundamental properties of the mammalian innate immune system revealed by multispecies comparison of type I interferon responses. PLoS Biol. 15, e2004086.
Simmen, K.A., Singh, J., Luukkonen, B.G., Lopper, M., Bittner, A., Miller, N.E., Jackson, M.R., Compton, T., Fruh, K., 2001. Global modulation of cellular transcription by human cytomegalovirus is initiated by viral glycoprotein B. Proc. Natl. Acad. Sci. U. S. A. 98, 7140–7145.
Stetson, D.B., Medzhitov, R., 2006. Type I interferons in host defense. Immunity 25, 373–381.
Vitour, D., Doceul, V., Ruscanu, S., Chauveau, E., Schwartz-Cornil, I., Zientara, S., 2014. Induction and control of the type I interferon pathway by Bluetongue virus. Virus Res. 182, 59–70.

Weiss, C.M., Trobaugh, D.W., Sun, C., Lucas, T.M., Diamond, M.S., Ryman, K.D., Klimstra, W.B., 2018. The interferon-induced exonuclease ISG20 exerts antiviral activity through upregulation of type I interferon response proteins. mSphere 3, e00209-18.
Wieland, S., Thimme, R., Purcell, R.H., Chisari, F.V., 2004. Genomic analysis of the host response to hepatitis B virus infection. Proc. Natl. Acad. Sci. U. S. A. 101, 6669–6674.
Zheng, Z., Wang, L., Pan, J., 2017. Interferon-stimulated gene 20-kDa protein (ISG20) in infection and disease: review and outlook. Intractab. Rare Dis. Res. 6, 35–40.
Zhou, Z., Wang, N., Woodson, S.E., Dong, Q., Wang, J., Liang, Y., Rijnbrand, R., Wei, L., Nichols, J.E., Guo, J.T., Holbrook, M.R., Lemon, S.M., Li, K., 2011. Antiviral activities of ISG20 in positive-strand RNA virus infections. Virology 409, 175–188.